2019-04

Phototactic tails: Evolution and molecular basis of a novel sensory trait in sea snakes

CroweRiddell, JM

10.1111/mec.15022
Molecular Ecology
Wiley

Phototactic tails: Evolution and molecular basis of a novel sensory trait in sea snakes

Running title: Phototactic tails in sea snakes

Jenna M. Crowe-Riddell[1,9*], Bruno F. Simões[1,2], Julian C. Partridge[3], David M. Hunt[3,8], Steven Delean[1], Julian G. Schwerdt[1], James Breen[4,5,6], Alastair Ludington[5], David J. Gower[7], Kate L. Sanders[1*]

[1]School of Biological Sciences, University of Adelaide, Adelaide SA 5005, Australia[2]School of Earth Sciences, University of Bristol, Bristol BS8 1TG, United Kingdom

[3]School of Biological Sciences and Oceans Institute, University of Western Australia, Crawley WA 6009, Australia

[4]Robinson Research Institute, University of Adelaide, North Adelaide SA 5006, Australia

[5]Bioinformatics Hub, University of Adelaide, Adelaide SA 5005, Australia

[6]South Australian Health & Medical Research Institute (SAHMRI), North Terrace, Adelaide SA 5000, Australia

[7]Department of Life Sciences, The Natural History Museum, London SW7 5BD, United Kingdom

[8]Centre for Ophthalmology and Vision Science, Lions Eye Institute, University of Western Australia, Nedlands WA 6009, Australia

[9]Department of Biology, University of Florida, Gainesville, FL 32611-8525, USA

*Corresponding authors: jenna.crowe-riddell@adelaide.edu.au, kate.sanders@adelaide.edu.au

Abstract

Dermal phototaxis has been reported in a few aquatic vertebrate lineages spanning fish, amphibians and reptiles. These taxa respond to light on the skin of their elongate hind-bodies and/or tails by withdrawing under cover to avoid detection by predators. Here, we investigated tail phototaxis in sea snakes (Hydrophiinae), the only reptiles reported to exhibit this sensory behaviour. We conducted behavioural tests in 17 wild-caught sea snakes of eight species by illuminating the dorsal surface of the tail and mid-body skin using cold white, violet, blue, green and red light. Our results confirmed phototactic tail withdrawal in the previously studied *Aipysurus laevis*, revealed this trait for the first time in *A. duboisii* and *A. tenuis*, and suggested that tail photoreceptors have peak spectral sensitivities between blue and green light (457-514 nm). Based on these results, and an absence of photoresponses in five *Aipysurus* and *Hydrophis* species, we tentatively infer that tail phototaxis evolved in the ancestor of a clade of six *Aipysurus* species (comprising 10% of all sea snakes). Quantifying tail damage, we found that the probability of sustaining tail injuries was not influenced by tail phototactic ability in snakes. Gene profiling showed that transcriptomes of both tail skin and body skin lacked visual opsins but contained melanopsin (*opn4x*) in addition to key genes of the retinal regeneration and phototransduction cascades. This work suggests that a non-visual photoreceptor (e.g. Gq rhabdomeric) signalling pathway underlies tail phototaxis, and provides candidate gene targets for future studies of this unusual sensory innovation in reptiles.

Keywords: extraocular, dermal phototaxis, sea snakes, dermal photoreception, melanopsin

Introduction

Most organisms use non-visual light detection to regulate essential physiological and behavioural functions (Wolken 1995). Prominent roles of non-visual photoreception include colour changes in the skin that facilitate camouflage, communication or thermoregulation, phototactic orientation and movement, and the circadian and seasonal timing of key biological events (Peirson et al. 2009; Foster & Soni 1998). Various cephalic or ‘extraocular’ tissues have been linked to non-visual photoreception,

such as the parietal organ and pineal complex (Foster & Soni 1998). In organisms lacking fur or feathers, the skin also provides a primary site for non-visual photoreception (Kelley & Davies 2016).

Dermal photoreception or the 'dermal light sense' mediates dermal phototaxis, defined here as the movement, including the whole body or a body part of an organism, towards or away from light (Kelley & Davies 2016; Steven 1963; Millott 1968). This sensory modality is best known among marine invertebrates, of which many species migrate along vertical light gradients and show abrupt withdrawal responses to sudden changes in light intensity (reviewed in Wolken 1988; Ramirez et al. 2011). Among vertebrates, dermal phototaxis have been described in lampreys (Young 1935; Steven 1950; Ronan & Bodznick 1991), hagfish (Patzner 1978; Steven 1955), aquatic salamanders, and a single frog (*Xenopus laevis* tadpole) (Alder 1976; Baker et al. 2015; Pearse 1910; Reese 1906; Sayle 1916). Olive sea snakes (*Aipysurus laevis*) are the only reptiles reported to show dermal phototaxis (Zimmerman & Heatwole 1990), but this species' phototactic behaviour is strikingly similar to that of the other elongate, aquatic vertebrates.

Sea snakes, lampreys, hagfish and aquatic salamanders all exhibit dermal photosensitivity that is most pronounced at the dorsal tips of their tails and stimulates negative phototaxis. Lamprey larvae and hagfish respond to tail illumination by deflecting their tails, swimming and/or burrowing to conceal themselves in river and lake beds (Ullén et al. 1993; Steven 1955; Deliagina et al. 1995; Young 1935; Binder & McDonald 2008; Patzner 1978). Resting olive sea snakes and aquatic salamanders respond with localised tail movements, often retracting their tail-paddles under reef or rock overhangs.

The convergent innovation of phototactic tails in elongate aquatic taxa that diverged relatively early in the >400 million-year evolutionary history of vertebrates suggests similar selection for concealment from predators. These selection pressures may be particularly strong in animals with vulnerable hind-bodies and tail paddles that are anatomically remote from the concentration of sensory organs on the head. Sea snakes have various predators, such as sharks and marine mammals, and specimens often have bite injuries to their tails, sometimes resulting in partial loss of the paddle (Heatwole 1975; Masunaga et al. 2008). Tail paddles are vital to efficient underwater locomotion so

tail damage must impact feeding, mating success and vulnerability to predation (Aubret & Shine 2008). Zimmerman and Heatwole (1990) demonstrated that captive *A. laevis* sea snakes concealed their tails under artificial reef during daylight more often than night, when tails were more likely to be protruding while the rest of the body was concealed. Hence, phototactic responses are expected to provide protection during daytime (and possibly dim-light) resting periods.

The genetic and physiological mechanisms underlying dermal phototaxis remain largely unknown for any vertebrate taxon (Kelley & Davies 2016). Hindering research progress is a conspicuous absence of photoreceptive structures such as stacked membranes or lenses within photoreceptive skin (Ramirez et al. 2011). However, gene expression studies have revealed visual opsins in colour-changing cells within the skin of cephalopods (Kingston et al. 2015; Ramirez & Oakley 2015; Mäthger et al. 2010), teleosts (Schweikert et al. 2018; Ban et al. 2005; Chen et al. 2013) and gekkonid lizards (Fulgione et al. 2014). This shows that the dermal photoreceptors involved in colour change likely evolved by co-opting existing visual photoreceptor pathways of the eye, despite lacking structures found in classical photoreceptors (Kingston & Cronin 2016; Ramirez et al. 2011). Other studies in teleosts (Bertolesi & McFarlane 2018) and amphibians (Provencio et al. 1998; Moriya et al. 1996) have identified a role for non-visual opsins in colour change, implying that independent, non-visual photoreceptor pathways underlie dermal photoreception in these diverse taxa.

In this study, we sought to better understand the evolution and molecular basis of tail phototaxis in sea snakes. We first used behavioural tests of tail (caudal) phototaxis in wild-caught sea snakes from eight species with the aim to better resolve the evolutionary origin of the trait. We then screened for candidate phototaxis genes expressed in the skin of two phototactic species. Because the dermal photoreceptive structures and genes involved in phototaxis are entirely unknown, we comprehensively profiled genes related to visual and non-visual photoreceptors in whole transcriptomes of tail and body skin, eye and other available organs. Finally, we quantified injuries on the tails of species with and without phototactic abilities, with the expectation that phototactic species might have lower bite rates indicating greater protection from attacks or have increased bite rates due to an intrinsically higher vulnerability to predation.

Materials and Methods

Specimens

Sea snakes are fully marine squamate reptiles that are phylogenetically nested within the Australo-Papuan terrestrial front fanged snakes (Elapidae: Hydrophiinae). Phototactic responses were measured in 17 wild-caught, captive individuals of eight species that spanned all major lineages of sea snakes: *Aipysurus laevis* (the only sea snake previously tested for phototactic behaviour), three other *Aipysurus* species, three *Hydrophis* species and one semi-aquatic species *Hydrelaps darwiniensis* (Supplementary materials; Table S1; ESM File 1). Tail injuries were recorded for a total of 111 museum specimens from two phototactic species, *A. laevis* (n = 39) and *A. duboisii* (n = 12), and two non-phototactic species *H. major* (n = 45) and *H. stokesii* (n = 15) (ESM File 2). The examined specimens were chosen from the same collection locality (Gulf of Carpentaria, Queensland, Australia) to minimise the effect of geographic variation in predation pressures; specimen information (snout-vent length, weight, sex and age) was available from (Fry G, personal communication).

Experiments and euthanasia were conducted in accordance with the Animal Ethics Committees of University of Adelaide (S-2015-119) and University of Florida (201502798) and specimens were collected and transported in accordance with Department of Parks and Wildlife of Western Australia licences to take fauna for scientific purposes (Permit #SF010002) and export fauna interstate (Permit #EA007665), Department of Environment, Water and Natural Resources of South Australia import permit (Permit #I12978) and from the Area de Conservación Arenal Tempisque (ACT) del Sistema Nacional de Areas de Conservación (SINAC), Costa Rica (No. ACT-OR-DR-055-17).

Behavioural experiments

Experimental set up

During experiments on *A. duboisii, A. laevis, A. tenuis* and *H. major* at the University of Adelaide, a snake was transferred from the seawater holding tank (24-28°C, 450L volume, 35 ppm, 12 h:12 h day:

night) to a round, black plastic behavioural arena (60 cm diameter × 60 cm height, 50 L volume) filled with seawater (24-28°C, 35 L volume, 13 cm depth) and covered by a mesh net. The arena was housed in a dark room lit by a single florescent red globe positioned 1 m above the arena (Figure S7). A lid was placed over the arena for 1-2 h to allow the snakes to adapt to the arena before initiating trials. Trials were recorded with a camera (GoPro Hero3+, Go Pro Inc., USA; 29.97 fps; 1920 × 1080) positioned above the behavioural arena. During experiments on *A. laevis, A. mosaicus, A. tenuis, H. darwiniensis, H. major, H. stokesii* and *H. platurus* at field sites, snakes were transferred to a rectangular, black plastic behavioural arena (66 cm length × 44 cm width × 23 cm height, 60 L volume) filled with freshwater (29 L, 10 cm depth) and covered by a mesh net. A lid was placed over the arena as described in experiments at the University of Adelaide, and trials were recorded directly by the observer and (where possible) with a camera (GoPro Hero3+, Go Pro Inc., USA; 29.97 fps; 1920 × 1080) positioned above the behavioural arena.

Light source

The light stimulus was delivered to localised areas of skin (Figure 4B) using a hand-held flashlight (UltraFire SH98 3-mode white light zooming, WhaFat Technological, Hong Kong) that incorporated a light-emitting diodes (LEDs) bulb that emitted white light with a spectral range of 300-900 nm. To test phototactic responses to different wavelengths of light, a hand-held flashlight (UltraFire 4-in-1 1-mode light) with interchangeable coloured LED bulbs was used to emit four colours: violet, blue, green and red of wavelengths of 393 nm, 457 nm, 514 nm and 623 nm, respectively. The flashlights were powered by two 7.4 volts rechargeable batteries (Fenix ARB-L3, Fenixlight, USA) that were re-charged after 6-12 trials to maintain a near-constant light output. At the start of each trial, the relative flashlight irradiance was measured using a PM100 digital optical power meter (Thorlabs, USA) and S210A UV-NIR thermal power head held 30 cm below the flashlight. Spectral and relative irradiance measurements are in Supplementary Materials (Figure S1).

Behavioural trials

Trials commenced after the snake had been inactive for at least 2 min. Experiments consisted of two to four sets of six trials, each trial being separated from the next by intervals of at least 1 h. Each snake was subjected to a mean of 17 trials over the course of the experiment. White light was shone on the dorsal surface of the tail skin ($T_{(s)}$) for duration of 5.3 s (± 1.30 s) at a distance of approximately 30cm. To control for the possibility that snakes responded to scattered light reaching the eyes, or the sight or sound of approaching experimenter, a white light was also shone on the dorsal surface of the mid-body skin ($B_{(s)}$) (Figure 1; Figure S7). Presentation of light was alternated between $T_{(s)}$ and $B_{(s)}$, and the order of presentation was reversed every set of six trials, for *A. duboisii* (*n* = 1), *A. laevis* (*n* = 4), *A. mosaicus* (*n* = 1), *A. tenuis* (*n* = 2), *H. major* (*n* = 1) and *H. platurus* (*n* = 2). In separate experiments, white light was presented only on $T_{(s)}$ in a single individual each of *A. laevis, A. tenuis, A. mosaicus, Hydrelaps darwiniensis, H. major* and *H. stokesii* (Table S1). *Aipysurus tenuis* (*n* = 2) appeared to be responsive to illumination of the body in addition to the tail, thus a new experiment was performed to test for phototactic response to body illumination in this species using an individual from *A. laevis* (*n* = 1) as a control. Experiments consisted of six sets of five trials in which white light was shone on the dorsal surface of the body at four locations (Table S2); light was presented sequentially along the body and the order of presentation was reversed between each trial set. A final experiment was conducted to test for sensitivity to different colours of light (violet, blue, green and red) in *A. tenuis* (*n* = 2) and *A. laevis* (*n* = 1).

Consistent with previous behavioural testing (Zimmerman & Heatwole 1990), a response was considered as 'negative phototaxis' if the part of the skin illuminated moved away from the light within 10 s and no other part of the snake moved. Behavioural responses were converted to a phototactic score to indicate whether a negative phototaxis occurred (Table 1) and mean response per species was calculated as a percentage (%) of trials in which phototaxis was observed. Latency to response was determined by viewing video footage of the phototactic response frame-by-frame (i.e. at 33.4 ms intervals) in GoPro Studio software v2.5.12 (CA, USA), and calculated as the difference between the time at which the light stimulus was switched on and the time at which the first phototactic movement of the snake occurred.

We mapped phototactic behaviour as a binary character (tail phototaxis absent or present) onto an existing phylogeny for sea snakes (Sherratt et al. 2018). Using these data, the most parsimonious interpretation of the origin of phototaxis in sea snake evolution was inferred by eye based on the assumption that gains and losses of this trait are rare and equally likely.

Transcriptome profiling

Tissue collection

Because the cellular structures responsible for light-sensing in the tails of sea snakes are unknown, we were unable to target specific locations in the skin for differential gene expression. Instead, we sampled the whole skin tissue (dermis, epidermis, beta layer) from three regions (two tail and one body) in two phototactic species and used whole transcriptome profiling to identify phototaxis genes. Seven skin samples were taken for RNA-sequencing: the photoreceptive tail tip of two *A. laevis* and one *A. tenuis*, putatively non-photoreceptive anterior ventral surface of the tail of a single *A. laevis* and *A. tenuis*, and the variably photoreceptive dorsal surface of the hind-body a short distance anterior of the vent of a single *A. laevis* and one *A. tenuis* (Figure 4B). In addition to the skin samples, we assessed the tissue-specificity of expression of genes related to photoreception by also sampling four non-skin tissues available from other projects: whole eye of *A. laevis*, and heart, testis and liver of the olive-headed sea snake *H. major* (Table S3).

Details of RNA extraction, sequencing, filtering and assembly

Tissues were homogenised using mortar and pestle in lysis buffer and grinder with liquid nitrogen before extracting total RNA (Roche Tissue RNA extraction kit). Library preparation and transcriptome sequencing for six skin tissues was performed by the Queensland Brain Institute Centre for Brain Genomics (QBI, Brisbane, Australia), for the eye by Beijing Genomics Institute (BGI, Shenzhen, China), and for one skin, testis, heart and liver by Australian Genome Research Facility (AGRF, Adelaide, Australia). Following RNA extraction (Roche Tissue RNA Extraction Kit) and quality control, dual indexed TruSeq libraries were generated and sequenced on an Illumnina HiSeq2000

machine (Illumina Inc., San Diego, CA) using V4 chemistry, producing 125 and 150 bp paired-end sequencing reads.

The quality of the raw reads was assessed using FastQC v0.11.4 (Andrews 2010), QUAST v4.5. (Quality Assessment Tool for Genome Assemblies; Gurevich et al. 2013), and using *ngsReports* v.0.99 (Ward et al. 2018) package in R. v3.4.2 (R Core Team 2017). Adapter sequences and low-quality reads were trimmed using AdapterRemoval v2.1.7 (Schubert et al. 2016) applying default quality parameters and a minimum sequence length of 20 bp. To reconstruct transcriptomes, *de novo* assembly was carried out the Trinity v2.5.1 pipeline (Grabherr et al. 2011; Haas et al. 2013) with default settings and a minimum contig length of 200 bp. Following transcript assembly, protein-coding regions were determined using TransDecoder v3.0.1. (Haas et al. 2013). Finally, assemblies were assessed for completeness, both by assessing the RNA read representation of the assemblies by aligning the trimmed reads back to their respective assemblies using Bowtie2 v2.2.9 (Langmead & Salzberg 2012) and by examining the presence of full-length protein-coding genes in the assemblies by searching against the SwissProt protein databases (The UniProt Consortium 2017) using BLAST+ (Camacho et al. 2009).

Unsupervised clustering of tissue samples was carried out using multi-dimensional scaling plots in R using the *edgeR* package v3.20.1 (Robinson et al. 2009) and log counts per million, with gene selection set to 'pairwise' for the top 500 genes. The intersections of expression levels among tissue samples were explored using the *UpSetR* package v1.3.3 (Lex et al. 2016).

Abundance estimates of genes

Estimated transcript abundances were generated using Salmon v8.2 (Patro et al. 2017), a pseudo-alignment program that quantifies gene expression without the need for direct genome alignments. RNA reads were mapped to a pitviper (*Protobothrops mucrosquamatus*) transcriptome (Aird et al. 2017), which was the best-annotated and closely related transcriptome currently available, and quantified reads were normalised using fragments per kilobase of transcript per million mapped reads (FPKM). To compare transcript abundance of genes related to photoreception among tissue samples,

FPKM counts were filtered by reference sequence gene categories (O'Leary et al. 2016) for predicted mRNA that are known to be involved in phototransduction and retinoid metabolism pathways of squamate reptiles (Schott et al. 2017) (Table S4). FPKM counts (Table S5) for visual genes were then log-transformed and a heatmap generated in R using the *pheatmap* package v1.0.8 (Kolde 2012) (ESM File 3).

Verifying the presence of genes related to visual and non-visual photoreceptors

Many vertebrate visual genes are part of large gene families that have high sequence similarity but include genes with non-visual functions (Porter et al. 2011). To verify the sequence identity of quantified transcripts with putative visual functions, we assessed the phylogenetic position of assembled sequences within maximum likelihood trees of visual genes from representative vertebrate groups (*Python molurus, P. mucrosquamatus, Thamnophis sirtalis, Pogona vitticeps, Gekko japonicus, Anolis carolinensis, Homo sapiens*). Transcripts nested within clades of vertebrate visual genes were considered to be verified visual genes. Conversely, if transcripts were recovered inside a clade of related genes with non-visual functions, these were considered to be erroneously mapped reads and indicated as such on the FPKM heatmap. Briefly, putative visual transcripts were located by custom nucleotide BLAST searches (Altschul et al. 1990) of assembled tissue transcriptomes (ESM File 4) with visual genes from representative vertebrate groups: squamates (*P. molarus, P. vitticeps, T. sirtalis, G. japonicus*), birds (*Gallus gallus*) and mammals (*Homo sapiens*), obtained from GenBank (Coordinators 2016). Significant nucleotide BLAST search hits (E-value < 1e-02; bit score > 200) were extracted from transcriptomes and aligned with representative vertebrate visual genes in Geneious v9.1.8 (Kearse et al. 2012) using a MUSCLE translation alignment v3.4 (Edgar 2004). Aligned sequences were checked for ambiguities and a maximum likelihood tree for each gene was built using RAxML v7.2.8 (Stamatakis 2006). We used an unpartitioned GTR GAMMA substitution model and the "rapid bootstrapping and search for best-scoring ML tree" algorithm with 1000 replicates. Trees were rooted by con-familial genes or, if tree was for a single gene only, a mammal gene sequence.

Quantifying tail injuries

Tail condition was recorded in museum specimens of sea snake (Figure S8). To evaluate the prevalence of tail injuries among the sampled species we used a hurdle model to examine 1) the presence of tail damage, and conditional upon damage occurring, 2) the number of tail injuries. The presence of damage was modelled assuming a binomial variance and logit link, and the count of tail injuries component of the model assumed a truncated Poisson variance and log link. We included the interaction between snout-vent length (cm) and species in our models because older (typically larger) snakes are expected to have more tail injuries and this relationship may differ between species. Snout-vent length (svl) was mean-centred for analysis. Other explanatory variables (sex, weight) were assessed using likelihood ratio tests. The likelihood of tail damage seen in non-phototactic species (*H. major* and *H. stokesii*) was compared to that observed in phototactic species (*A. laevis* and *A. duboisii*) using planned contrasts (Torsten et al. 2008). These analyses were conducted in R using additional packages *multcomp* v1.4.8 (Bretz & Westfall 2014) and *countreg* v0.2 (Zeilies et al. 2008).

Results

Evidence for dermal phototaxis in eight species and evolutionary origin in sea snakes

Our behavioural tests provided evidence of negative tail phototaxis in all individuals of *Aipysurus laevis, A. tenuis* and *A. duboisii* (tail withdrawals in response to white LEDs, 100%, 87% and 70% of trials, respectively), but not in any of *A. mosaicus* (5%), *Hydrophis major* (3.2%), *Hydrelaps darwiniensis, Hydrophis stokesii* or *H. platurus* (Figure 1A). Consistent with previous observations in *A. laevis* (Zimmerman & Heatwole 1990), tail phototaxis in individuals of *A. laevis, A. duboisii* and *A. tenuis* was a stereotyped movement of the tail towards the centre of body mass and away from the light stimulus (Table 1; ESM File 5). Tail latencies recorded for the three phototactic species showed that tails moved within 7 seconds (s) of illumination. Mean response times were 2.1 s for *A. tenuis*, 2.5 s for *A. duboisii* and 3.4 s for *A. laevis* (Figure 1B), and the shortest tail latencies recorded for each species were 0.25 s for *A. tenuis*, 0.55 s for *A. laevis* and 1.05 s for *A. duboisii* (Figure 1B). To control

for the effects of the experimenter and to test for phototactic responses to scattered light reaching the eyes, trials of tail response were alternated with trials of white light shone on the mid-body (instead of tail). This was done for 11 individuals of six species, and yielded no phototactic responses to mid-body illumination in *A. duboisii*, *A. mosaicus*, *H. major* and *H. platurus*, and low response rates in *A. tenuis* (9% of 11 trials, $n = 2$) and *A. laevis* (2.8% of 36 trials, $n = 5$) (Figure 1A).

To test preliminary observations of phototactic responses to hind-body illumination in *A. tenuis*, a separate experiment was performed on *A. tenuis* ($n = 2$) and *A. laevis* ($n = 1$). Here, phototaxis was also recorded in response to white LED light shone on four dorsal regions along the body axis. *Aipysurus tenuis* showed a stereotyped withdrawal (movement of the illuminated part of the body towards the centre of body mass and away from the light stimulus; ESM File 6) in response to illumination of the dorsal skin on the hind-body (pre-vent, 66.7% of 12 trials), posterior mid-body (16.7% of 12 trials), anterior mid-body (16.7% of 12 trials) and neck region (22.1% of 13 trials), but at a comparatively lower rate compared to tail illumination (100% of 12 trials; ESM File 6). In contrast, no phototactic responses were recorded in any of the four regions of body skin in *A. laevis*.

For phototactic species *A. tenuis* and *A. laevis*, we compared latencies of responses to tail illumination from four different wavelengths of light produced by LEDs having approximately equal intensities. The results suggest peak sensitivities of tail photoreceptors between 457 and 514 nm (Figure 2); but this pilot experiment did not allow us to generate full response curves for spectral sensitivity or latency of tail movement because only four wavelengths were tested. Relative irradiance measurements for the white, violet, green, blue and red light are shown in Figure S1.

Based on the results of our behavioural tests, and an expectation that evolutionary gains and losses of phototaxis are rare and equally likely, the most parsimonious inference is that this sensory modality evolved in the ancestor of a clade of six *Aipysurus* species: *A. laevis, A. fuscus, A. tenuis, A. duboisii, A. foliosquama* and *A. apraefrontalis* (Figure 3). An alternative scenario under which phototaxis evolved in the common ancestor of all *Aipysurus* and was lost on the lineage leading to *A. mosaicus* involves one additional step. Hence, pending future studies of additional *A. mosaicus* individuals and key taxa such as *Emydocephalus* and *Ephalophis-Parahydrophis* (indicated by

asterisks on Figure 3), we tentatively infer a single origin of phototaxis within *Aipysurus*, and an absence of this trait in all other sea snakes (i.e. 90% of species, including the ~50 *Hydrophis* species).

Expression of genes related to visual and non-visual photoreceptors

Assembled transcriptomes for sea snake eye, heart, liver, testis and seven skin tissues were profiled for genes relating to visual and non-visual photoreceptors (Table S3; S4). Five vertebrate phototransduction genes were not detected in the eye transcriptome (*sws2, rho2, grk1, gnat1, gucy2F, pde6a, pde6h*). This is consistent with previous genomic and transcriptomic studies that suggest these genes are missing in snake genomes, hence they were not profiled in the remaining tissue transcriptomes. Summary statistics for sequencing, assembly and transcript completeness are given in Table 2, Table 3 and Supplementary Results (Figure S2). Multidimensional scaling plots and overall expression profiles for tissue transcriptomes are also given in Supplementary Results (Figure S3; S4; S5).

Opsins

Three genes encoding for visual opsins (*opn1sw, rho1, opn1lw*) were detected in *A. laevis* eye, and a single visual opsin (*opn1sw*) was detected in *H. major* testis (Figure 4). Genes for two non-visual opsins were also expressed: *xenopus-like* melanopsin (*opn4x*) was detected in *A. laevis* eye, *H. major* testis and two skin transcriptomes each from *A. laevis* and *A. tenuis*. Neuropsin (*opn5*) was expressed in *A. laevis* eye, *H. major* testis and a single skin transcriptome from *A. laevis* (Figure 4).

Phototransduction

A total of 24 genes related to phototransduction in visual photoreceptors of vertebrates (i.e. ciliary genes) were detected in the *A. laevis* eye, 17 in *H. major* testis, nine in *H. major* heart, seven in *H. major* liver and 13 across *Aipysurus* skin tissues (Figure 4). There was no discernible co-expression pattern between putatively photoreceptive skin and variably or non-photoreceptive skin (Figure 4). Phototransduction genes detected in the majority (four or more) of skin tissue samples were *arrb2, gna11, guca1b, pdc-like, pdc-likeb1, pdc-likeb3, pde6d,* and *pde6g* (Figure 4). Genes *grk7-like* and

grk5 were detected in a single skin transcriptome each from *A. laevis* and *A. tenuis*, and *sag* in a single skin transcriptome from *A. tenuis* (Figure 4). Phototransduction genes *grk5, guca1a/c, pdc, gnat2, sag,* and *rcvrn* were detected in the skin using FPKM levels, but gene tree analyses indicated that these are most likely homologous with *grk5-like*, *guca1b, pdc-like2/3, gnai2/3, arrestin C-like*, and *hippocalcin-like* (*hpcl-like),* respectively (ESM File 7). The following 11 phototransduction genes were not detected in skin transcriptomes: *cnga3, cngb1, cngb3, gnat2, guca1a, guca1c, gucy2d-like, pdc, pdc-like2, pde6b-like, pde6c* and *slc24a2* (Figure 4; ESM File 7). Genes related to phototransduction in non-visual photoreceptors (e.g. intrinsically-photoreceptive retinal ganglion cells; ipRGCs) and invertebrate visual photoreceptors (i.e. rhabdomeric genes), *gna11, plcb1, plcb3, plcb4,* were also profiled and found to be widely expressed across all organs including skin (data not shown).

Retinoid regeneration

A total of 13 genes related to retinoid regeneration were detected in the *A. laevis* eye, eight in *H. major* testis, nine in *H. major* heart, seven in *H. major* liver, and eight across *Aipysurus* skin tissues (Figure 4). There was no discernible co-expression pattern between putatively photoreceptive skin and variably or non-photoreceptive skin (Figure 4). Genes detected in the majority (more than four) skin tissues were *lrat, rdh8-like, rdh10, rdh11-like, rdh12-like, rdh14,* and *rpe65*, and the gene *rgs9bp* was detected in two skin tissues from *A. laevis* (Figure 4). The identity of some retinoid regeneration genes that were detected in the skin tissues using FPKM levels (*rhd5* and *rgs9*) could not be verified by custom nucleotide BLAST searches and phylogenetic analysis (ESM File 7). The following retinoid regeneration genes were not detected in skin transcriptomes: *abca4, rbp3, rdh5, rgr and rgs9*.

The relationship between tail damage and phototactic ability

Phototactic species *A. laevis* and *A. duboisii* had slightly higher proportions of damaged tails (67% and 58 %, respectively) compared to non-phototactic species *H. major* (47%) and *H. stokesii* (40%) from the same geographic location (Gulf of Carpentaria, Australia) (Table S6). We predicted that phototactic ability (i.e. species) would explain differences in the likelihood of tail damage occurring. However, there was no effect of species on likelihood of tail damage ($\chi_2 = 2.5$, $P = 0.47$; Table S7).

There was a positive relationship between body length (measured from the snout to the vent: svl) and the probability of tail damage; 10cm increases in svl nearly doubled the likelihood of tail damage (1.97-fold increase, 95% confidence interval 1.26-3.27; $\chi_2 = 10.9$, $P = 0.001$; Table S7; Figure S6). This relationship was consistent across all the species sampled (i.e., no species *svl interaction; $\chi_2 = 1.4$, $P = 0.69$). We therefore found no evidence for our *a priori* hypothesis of differences in the likelihood of tail damage between non-phototactic (*H. major* and *H. stokesii*) and phototactic species (*A. laevis* and *A. duboisii*; Table S8). Furthermore, conditional on damage occurring, there was no evidence for differences in the number of injuries between species ($\chi_2 = 5.4$, $P = 0.14$) or associated with size (i.e., svl; $\chi_2 = 0.05$, $P = 0.9$; Table S7).

Discussion

Our study presents substantial new data on a novel sensory trait that is underexplored in vertebrates. The difficulties inherent in collecting and housing live sea snakes meant that we were unable to extensively replicate behavioural experiments. However, our tests of 17 individuals of eight species yielded highly consistent results with low variability both within individuals and among individuals within species. These results confirm the phototactic ability of the only previously studied species of reptile (the olive sea snake, *Aipysurus laevis*) and reveal this trait for the first time in *A. duboisii* and *A. tenuis* (Figure 1; ESM File 5). We recorded phototactic responses of the hind-body in *A. tenuis* that have not previously been reported and may be linked to the elongate body form of this species (thus increased distance between the hind-body and cephalic sensory organs). All other species tested showed little or no response to light on the body skin, which suggests that photoreceptive regions are primarily located in the tail skin.

We found that snakes were most responsive to blue and green light, and least responsive to violet and red. Considering the narrow bandwidth and the approximately balanced in light output (at least, in energy terms) of the coloured LEDs, we suggest that dermal photoreceptors have spectral sensitivities between 457 and 514 nm (the peaks of the blue and green LEDs). Such a spectral location is consistent with the spectral sensitivities of other dermal photoreceptors such as chromatophores in cephalopods

(470–-480 nm; Ramirez and Oakley 2015) as well as that of our candidate non-visual opsins (e.g. melanopsin; Díaz et al. 2016; Bertolesi and McFarlane 2018). However, our pilot experiment lacks the necessary spectral resolution that would allow us to distinguish melanopsin-based photoreception, with a peak sensitivity typically around 480nm, from that of rhodopsins (with peak sensitivities generally around 500 nm). Latencies recorded for sea snake tails were comparable to hagfish and lampreys, i.e. between one and six seconds (Newth & Ross 1954; Steven 1955).

Based on an expectation that losses and gains of phototaxis are rare, we offer a preliminary hypothesis that this sensory modality originated in the ancestor of a clade of six *Aipysurus* species (Figure 3). To better resolve the origin of phototaxis, future studies will be needed to increase individual sampling (particularly of putatively non-phototactic *Aipysurus*, i.e. the *A. mosaicus* species complex), and target key lineages such as *Emydocephalus* and *Ephalophis-Parahydrophis.* Nevertheless, the absence of phototactic responses in six individuals from four species that are widely distributed in the large *Hydrelaps-Hydrophis* clade suggests that most of the > 60 known sea snake species lack phototactic tails, prompting the question of why only some sea snakes have evolved (or retained) this sensory behaviour.

Numerous species traits must influence vulnerability to predation and/or the locomotory costs of tail damage, including diel and spatial activity patterns, preferred habitat and depth, and size of body and tail. *Aipysurus* species have smaller geographic ranges and stronger patterns of mitochondrial geographic structure compared to *Hydrophis* (Nitschke et al. 2018); these observations indicate lower dispersal propensities in *Aipysurus*, which might result in slower swimming speeds and thus stronger selection for strategies for crypsis such as tail phototaxis. However, there is no particular trait, or combination of traits, that solely characterizes the species shown (or inferred) in our study to have phototactic tails. All sea snakes have paddle-shaped tails used for locomotion, and all species are active foragers that rest at times during the day, often under coral or rocky overhangs (Rasmussen et al. 2011). Furthermore, we found no difference in the likelihood of tail damage or in the total number of injuries sustained by phototactic *A. laevis* and *A. duboisii* compared to the non-phototactic *H.*

stokesii and *H. major*, which suggests that there is no intrinsically higher (or lower) vulnerability to predation in the phototactic populations sampled. The *Aipysurus-Emydocephalus* and *Hydrophis* clades, however, show notable differences in their adaptations to marine habits, including use of different tissues to seal the mouth and different vertebral processes to support their tail paddles (Sanders et al. 2012). Hence, a recent origin of tail phototaxis in just the *Aipysurus-Emydocephalus* clade might be best explained by historical contingency, rather than an absence of similar selection pressures in other sea snakes.

Candidate genes underlying dermal phototaxis

The conspicuous absence of classical visual photoreceptor structures in the skin of phototactic sea snakes, lampreys, hagfish and aquatic amphibians poses a significant challenge to research on vertebrate dermal photoreception. Based on our expectation that tail phototaxis could be mediated by independent or novel genetic pathways, we decided to screen whole skin transcriptomes for genes related to visual and non-visual photoreceptors. This approach yielded genes of interest in the eye of sea snakes and low expression abundance and variably non-specific patterns of expression across tissue types (Figure 4; Table S5). Below we discuss a putative role for these candidate genes in a non-visual photoreceptor pathway in sea snake skin.

Light detection pathways begin with light-absorbing pigments such as the visual opsins that are expressed in the classical retinal photoreceptors, rods and cones, and are also implicated in dermal photoreception in cephalopods (Kingston & Cronin 2016; Ramirez & Oakley 2015), teleosts (Schweikert et al. 2018; Chen et al. 2013) and gekkonid lizards (Fulgione et al. 2014). Absorption of light by opsins initiates a complex phototransduction cascade in which the chromophore retinaldehyde (vitamin A) bound with the opsin must photoisomerize from a *cis* to an *all-trans* conformation. In visual opsin systems, photoisomerization then activates phosphodiesterase-6 (PDE6) through coupling with a heterotrimer G protein 'transducin' (GNAT), producing a hyperpolarising current by the opening of cyclic-nucleotide gated channels (CNG) in the photoreceptor membrane (Figure 5A).

As expected from transcriptomic and genomic studies of vision in snakes, several phototransduction genes (*grk1, gnat1, gucy2F, pde6a, pde6h*) and two visual opsin genes (*sws2* and *rho2*) were absent in the *A. laevis* eye transcriptome (Bhattacharyya et al. 2017; Davies et al. 2009; Hart et al. 2012; Hauzman et al. 2017; Schott et al. 2015; Schott et al. 2017; Simões et al. 2016). All three of the visual opsins found in snakes *(opn1lw, opn1sw* and *rho1*) were detected in the *A. laevis* eye, but none were detected in the skin of *A. laevis* or *A. tenuis* (Figure 4). Consistent with the absence of a visual opsin to absorb light, only a few vertebrate phototransduction genes were present in the skin, and together these genes form an incomplete phototransduction cascade for image-forming vision (Figure 5A). Importantly, we did not detect transcripts for GNAT (*gnat2*), PDE6 rod-specific units (*pde6b*) and regulator of G-protein signalling 9 (*rgs9*). However, 13 visual phototransduction genes were found to be expressed in the skin of sea snakes (Figure 4), providing to a shortlist of genes that might be involved in independent, non-visual photoreceptor pathways (Figure 5).

We detected in the skin two candidate light-absorbing pigments for initiating tail phototaxis in sea snakes: 'xenopus-like' melanopsin (*opn4x)* and neuropsin *(opn5)* (Figure 5C) are vertebrate genes associated with a range of non-visual protein functions and patterns of tissue-specific expression. Neuropsin is present in the brain and skin of vertebrates, and is thought to play a role in retinal photoentrainment, changes of skin colour in fish (Buhr et al. 2015; Schweikert et al. 2018) and dermal phototaxis in *Xenopus* tadpoles (Currie et al. 2016). The 'mammal-like' class of melanopsin (*opn4m*) is present in the ipRGCs of the eye (Provencio & Warthen 2012; Bellingham et al. 2006) and some cranial nerves (Matynia et al. 2016), and has a range of photosensory functions including photoentrainment of molecular clocks, local pupil light reflex, DNA repair and melatonin synthesis (reviewed in Peirson et al. 2009; Bertolesi and McFarlane 2018). The role of *opn4x* is understudied but it is expressed in a wide range of tissues including the brain and eye of fish, amphibians, reptiles, turtles and birds (reviewed in Davies et al. 2014). Because *opn4x* is expressed in dermal melanophores of fish and amphibians (Oshima 2001; Bertolesi & McFarlane 2018; Provencio et al. 1998) and neuromasts of the lateral line system in *Xenopus* tadpoles (Baker et al. 2015) it is a good candidate

pigment for non-visual light detection pathways in non-mammalian vertebrates such as sea snakes (Kelley & Davies 2016).

The pathways interacting with *opn4x* are incompletely known, but the gene is similar in DNA sequence and function to opsins that use phototransduction pathways of invertebrate photoreceptors (i.e. rhabdomeric) (Graham et al. 2008; Isoldi et al. 2005; Díaz et al. 2016). Following photoisomerization, melanopsin is thought to activate a G-protein Gq/11 (GNAQ / GNA11) and phospholipase C (PLC) second messenger cascade, producing depolarizing currents by the activation of TRP-like channels (TRP) (Díaz et al. 2016). We detected genes that encode the primary proteins in the putative melanopsin pathway, GNAQ (*gnaq*) and PLC beta (*plcb1*, *plcb3*, *plcb4)*, across a range of sea snake tissues including skin (data not shown), suggesting that some type of Gq rhabdomeric signalling pathway is possible for melanopsin-based dermal photoreception in sea snakes. However, these genes are also integral to a range of cellular pathways, so further molecular studies are needed to confirm their role in tail phototaxis. If *opn4x* is indeed responsible for mediating phototaxis in sea snakes, previous studies of *opn4x* expression (Baker et al., 2015; Davies et al., 2014; Provencio et al., 1998) would suggest three candidate cell types that may be associated with dermal photoreceptors: 1) dermal melanophores involved in colour change, 2) dermal mechanoreceptors, and 3) peripheral nerve endings in the epidermis that may or may not be associated with dermal mechanoreceptors. Given that dermal phototaxis is not linked to colour change in sea snakes, we suggest that future studies are most likely to find photoreceptive structures in either peripheral nerve endings in the epidermis or dermal mechanoreceptors, or a combination of both.

The phototransduction cascade is completed with the regeneration of *all-trans*-retinaldehyde to supply new *cis*-retinaldehyde to the opsin, which involves retinal pigment epithelium 65 Da (RPE65), lecithin retinol acyltransferase (LRAT) and various retinol dehydrogenase (RDH) proteins (Figure 5B). We detected seven genes involved in retinal regeneration that were widely expressed across *Aipysurus* skin and *Hydrophis* tissues (Figure 5B), including *rpe65*, the expression of which is generally thought to be restricted to the retinal pigment epithelium and cone photoreceptors of the eye (Wright et al. 2015). *Rpe65*, in conjunction with *lrat* (also expressed in the tail skin), has a key role in

isomerization of the opsin chromophore (Wright et al. 2015; Saari 2012). Although the *opn4m* has an intrinsically photoisomerizing (i.e. bistable) function, light stability in *opn4x* is variably monostable or bistable depending on the isoform and/or taxon (Díaz et al. 2016; Tu et al. 2006). Significantly, associated retinal regeneration proteins of the eye, *rlbp1* and *rgr*, are absent from *Aipysurus* skin tissues. Although the operation and interaction of *opn4x* and/or *opn5* with *rpe65 and lrat* (and other retinal regeneration genes) within the skin is not entirely clear, a role in the regeneration of opsin chromophore in dermal photoreceptors would seem likely.

Conclusions

Our sea snake skin transcriptomes yielded non-visual opsins (and an absence of visual opsins), in addition to several phototransduction and retinal cycle genes, providing preliminary evidence that tail phototaxis may be mediated by genes related to non-visual photoreceptors that do not involve image-forming vision but rather provide information on overall light levels in the environment. Although future studies are needed to confirm a functional role of our candidate genes in mediating tail phototaxis, and uncover the precise location of photoreceptive structures in sea snake skin,these findings highlight the utility of gene expression profiling as a first step in identifying the molecular mechanisms underlying sensory evolution. Dermal phototaxis may be more prevalent in vertebrates than currently recognised. We suggest that it is likely to be particularly important for aquatic or burrowing taxa with elongate bodies and/or tails that are anatomically remote from the concentration of sensory organs on their heads. Transcriptome profiling studies in other reptiles (including putatively non-phototactic sea snakes) should target skin to identify patterns of taxon- and tissue-specific expression of genes related to visual and non-visual photoreceptors.

Acknowledgements: This work was supported by a Hermon-Slade Foundation Grant (HSF0001039517), The University of Adelaide Environment Institute Seed Grant, and Australian Research Council (ARC) Future Fellowship (FT130101965) to K.L.S and ARC Discovery Project (DP180101688) to B.F.S., D.M.H., J.B. and K.L.S.; a Leverhume Grant (RPG-342) to D.J.G., D.M.H.

and J.C.P.; an Australian Government Research Training Program Scholarship and Fulbright Postgraduate Scholarship held by J.M.C-R.; and a European Union Marie Skłodowska-Curie Global Fellowship (GA703438) to B.F.S. Specimen SVL, weight, and sex data used in analyses of tail injuries were supplied by CSIRO Oceans and Atmosphere, Brisbane. We are grateful to Kylie Sherwood (Chelonia Broome), Harvey Lillywhite, Coleman Sheehy III, Mark Sandfoss, Ruchira Somaweera, Mick and Kelly Woodley and crew (Absolute Ocean Charters, Broome) for assistance in catching and transporting sea snakes. We thank Jack Jones, Dan Tucker, Lucille Chapuis, Caroline Kerr and Ralph Foster for advice in aquaria set up. We thank Adrian Giffen and Murray Hamilton for the use of a power meter and light sensor. For ac- cess to specimens and laboratories, we thank Mark Hutchinson and Carolyn Kovach (South Australian Museum), Andrew Amey and Patrick Couper (Queensland Museum), and Jodi Rowley and Stephen Mahony (Australian Museum).

Data accessibility: Supplementary materials, results, tables and figures attached separately. Raw RNA-reads are available at NCBI Sequence Read Archive (SUB4931382). Electronic supplementary data are available at Figshare (DOI: 10.25909/5c1ade89814b0) including:

- **ESM File 1:** Beh-exp.xlsx containing raw and summary data for behavioural experiments of 17 individuals from eight species of sea snake.
- **ESM File 2:** Tail-beh-injuries.xlsx containing raw data of tail damage in museum specimens of sea snakes.
- **ESM File 3:** FPKMheatmap.zip containing R script for generating MDS plot & FPKM heatmap, TPM matrix for each sea snake transcriptome created using Salmon
- **ESM File 4:** TranscriptomeAssemblies-PhototacticTails-skin-heart-liver-eye-testis.zip containing transcriptomes for sea snake tissues assembled using Trinity pipeline.
- **ESM File 5:** Video containing examples of tail phototaxis in sea snakes
- **ESM File 6.** Video containing examples of body phototaxis in sea snakes.

- **ESM File 7.** RAXML-gene-trees.zip containing maximum likelihood gene trees in fasta and nexus format shows relationship among putative phototaxis sea snake transcripts and phototaxis genes from representative vertebrate lineages.

Author contributions: J.M.C.-R. and K.L.S conceived of the study. J.M.C.-R. and K.L.S conducted field work and behavioural experiments. J.M.C.-R., K.L.S, B.F.S. and D.J.G. collected tissues. A.L., J.B. and J.G.S. generated summary statistics for mRNA reads. J.G.S. assembled transcriptomes. J.B. conducted read quantification. J.M.C.-R. and A.L. conducted gene profiling with input from B.F.S., D.J.G. and K.L.S. Phylogenetic analyses for gene verification was performed by J.M.C.-R. with input from B.F.S. and K.L.S. Tail injuries were quantified by J.M.C.-R. and analysed by S.D. The manuscript was written by J.M.C.-R. and K.L.S. with significant input from all co-authors. The authors declare no competing interests.

Tables

Table 1: Categories of behavioural responses to light on the skin. Phototactic scores were negative phototaxis = 1 and no phototaxis = 0.

Category	*Description of behaviour*	*Phototactic score*
CW	Tail withdraws completely out of light within 10 s and no other part of snake moves	1
W	Tail withdraws away from light within 10 s and no other part of snake moves	1
TL	Tail tilts from dorsal plane to sagittal plane within 10 s and no other part of snake moves	0
TJ	Sudden movement of tail only	0
BJ	Sudden movement of body only	0
B	Body undulates as in swimming movement	0
HT	Head moves to location of tail, tail may or may not withdraw	0
BW	Body withdraws away from light within 10 s and no other part of snake moves	1
NR	No response, body and tail do not change position	0

Table 2. Statistical summary of sequencing.

558

Species	ID	Phototactic region	Paired end raw reads	% Removed	Trimmed reads	Reads mapped	% Alignment
Aipysurus laevis	KLS0459	Eye	41,960,313	0	41,960,313	37,485,594	89.3
		Skin photoreceptive tail tip (dorsal)	30,343,697	37.9	18,839,010	18,377,480	97.6
	KLS0656	Skin photoreceptive tail tip (dorsal)	16,098,369	43.6	9,082,453	8,060,311	88.7
		Skin non-photoreceptive tail (anterior)	17,696,227	28.8	12,601,077	11,943,910	94.8
		Skin non-photoreceptive body near vent (dorsal)	27,845,728	36.8	17,588,152	16,791,799	95.5
Aipysurus tenuis	KLS0654	Skin photoreceptive tail tip (dorsal)	20,397,990	52.0	9,798,407	8,841,047	90.2
		Skin non-photoreceptive tail (anterior)	31,707,833	32.2	21,486,415	20,745,575	96.6
		Skin photoreceptive body near vent (dorsal)	16,828,408	32.1	11,428,795	10,375,249	90.8
Hydrophis major	KLS0460	Heart	31,189,072	41.0	18,392,676	17,928,884	97.5
		Liver	31,187,724	39.8	18,782,654	18,265,069	97.2
		Testis	27,457,192	40.4	16,371,706	15,700,688	95.9

559
560
561 **Table 3.** Summary statistics of Trinity assemblies.
562

Specimen			*Contigs*	*Length*			*Contigs >= 1000 bp*		*Contigs >= 5000 bp*		*Contigs >= 10000 bp*		
Spp.	*ID*	*Tissue*	*No. assembled*	*Total length (bp)*	*Longest contig (bp)*	*N50 contig length (bp)*	*No.*	*%*	*No.*	*%*	*No.*	*%*	*GC %*
A. laevis	KLS 0459	Eye	230,892	80,614,082	18,092	2,806	24,256	10.5	2,721	1.2	130	0.06	42.3
		Skin photoreceptive tail tip (dorsal)	130,893	70,608,010	21,767	2,164	24,074	18.4	1,163	0.9	21	0.02	42.7
	KLS 0656	Skin photoreceptive tail tip (dorsal)	49,779	5,155,121	8,160	814	1,223	2.5	11	0.0	0	0.00	43.6
		Skin non-photoreceptive tail (anterior)	90,353	23,528,511	10,860	1,121	7,786	8.6	50	0.1	2	0.00	44.7
		Skin non-photoreceptive body near vent (dorsal)	159,456	63,237,696	14,787	1,784	21,986	13.8	708	0.4	20	0.01	44.4
A. tenuis	KLS 0654	Skin photoreceptive tail tip (dorsal)	76,189	7,419,783	8,560	780	1,643	2.2	4	0.0	0	0.00	42.7
		Skin non-photoreceptive tail (anterior)	118,552	44,671,944	10,895	1,478	16,550	14.0	144	0.1	4	0.00	44.4
		Skin photoreceptive body near vent (dorsal)	92,552	14,741,471	10,723	892	4,120	4.5	21	0.0	2	0.00	44.4
H. major	KLS 0460	Heart	124,657	68,064,584	51,061	1,995	23,763	19.1	820	0.7	18	0.01	42.9
		Liver	125,968	49,361,792	19,451	1,595	18,496	14.7	178	0.1	8	0.01	42.8
		Testis	200,649	92,040,799	11,282	1,743	32,250	16.1	784	0.4	5	0.00	43.1

563

Figures

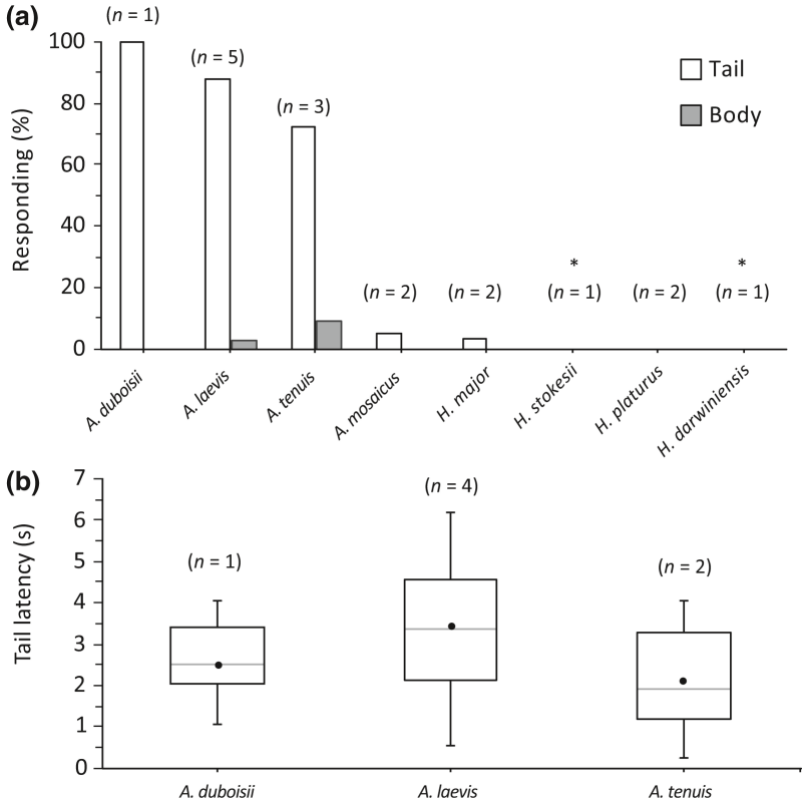

Figure 1. Negative phototaxis in response to white LED light on the dorsal surface of skin in sea snakes. 'Negative phototaxis' was recorded if the illuminated region moved away from the light within 10 s and no other part of the snake moved. A) Response (%) to light on tail skin and body skin in eight species; asterisks indicate species in which light was shone on the tail skin only. B) Tail latency in the phototactic species; box plots represent median (middle solid horizontal line), mean (black dots) and range (dotted line) of latencies across a mean of 6 trials per individual.

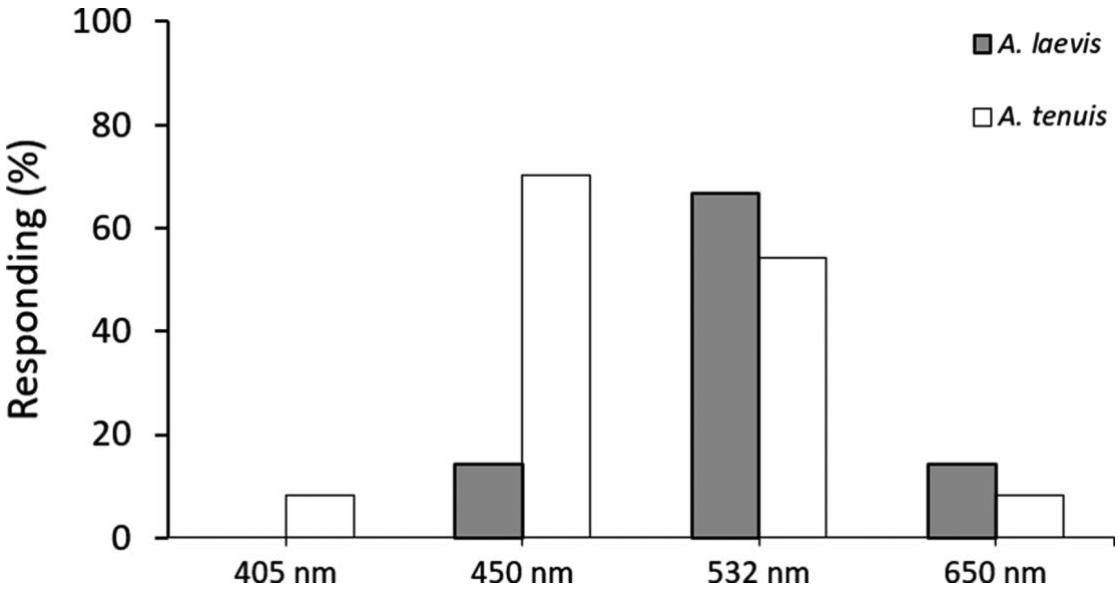

Figure 2. Negative tail phototaxis in response to four coloured LED lights, violet (392 nm), blue (347 nm), green (514 nm) and red (623 nm), in three captive individuals from two species, *Aipysurus laevis* (n = 1) and *A. tenuis* (n = 2), across a mean of 6 trials per individual. 'Negative phototaxis' was recorded if the illuminated region moved away from the light within 20 s and no other part of the snake moved.

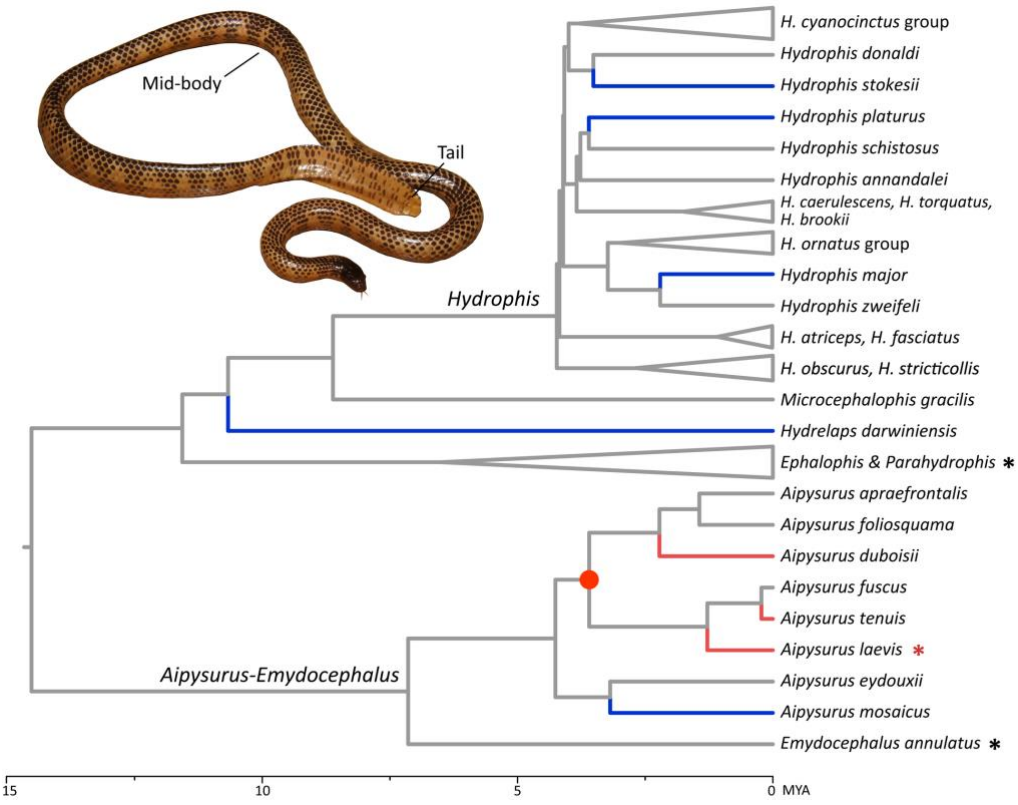

Figure 3. Phylogenetic tree of sea snakes showing distribution of tail phototaxis: red branches represent species that showed phototactic responses to localised white light on the tail but not the mid-body, blue branches represent species that were unresponsive to localised white light on both the tail and mid-body, and untested species are shown as grey branches. Based on these currently available data (17 individuals of 8 species), the most parsimonious inference is that tail phototaxis evolved in the ancestor of a clade of six *Aipysurus* species (the node marked with a red dot). The only previously studied species, *Aipysurus laevis*, is indicated by red asterisk. Tree modified from Sherratt et al., (2018); legend is in millions of years ago (MYA); image of *Aipysurus tenuis* shows regions that were tested for phototactic responses, taken with permission from Mirtschin, Rasmussen, & Weinstein (2017).

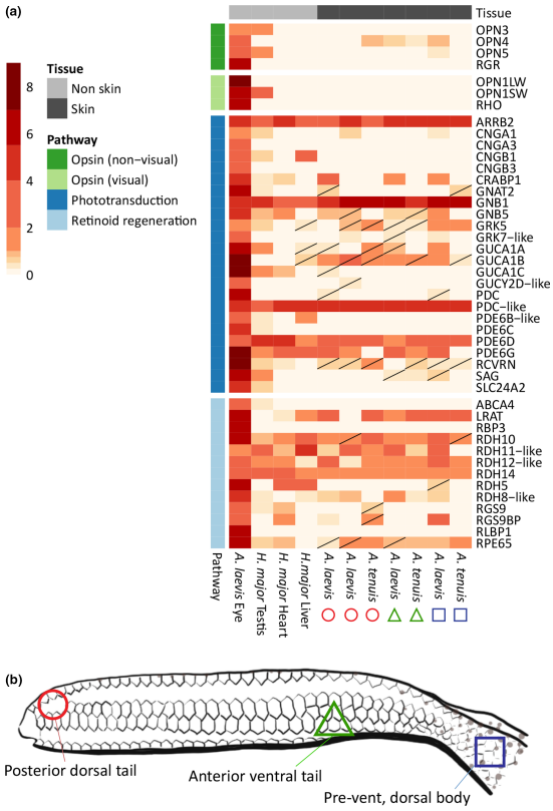

Figure 4. Gene profiling of tissue transcriptomes from *Aipysurus laevis*, *A. tenuis* and *Hydrophis major* sea snakes. A) Heatmaps show normalised expression levels of genes for visual pigments (opsins), phototransduction cascades related to visual photoreceptors and retinoid regeneration. RNA reads were quantified by pseudoalignment to a pitviper (*Protobothrops mucrosquamatus*) transcriptome; fragments per kilobase of transcript per million mapped reads (FPKM) were log-transformed for visualising in heatmap; strikethrough cells indicate transcripts whose visual function could not be verified by nucleotide BLAST searching and phylogenetic analysis (ESM File 7). B) Schematic diagram of tail showing where skin tissues were collected from phototactic species (*A. laevis* and *A. tenuis*). Putative dermal light sensitivity is indicated by red circle (photoreceptive), green triangle (non-photoreceptive) and blue square (photoreceptive in *A. tenuis* only). Diagram modified from Zimmerman and Heatwole (1990).

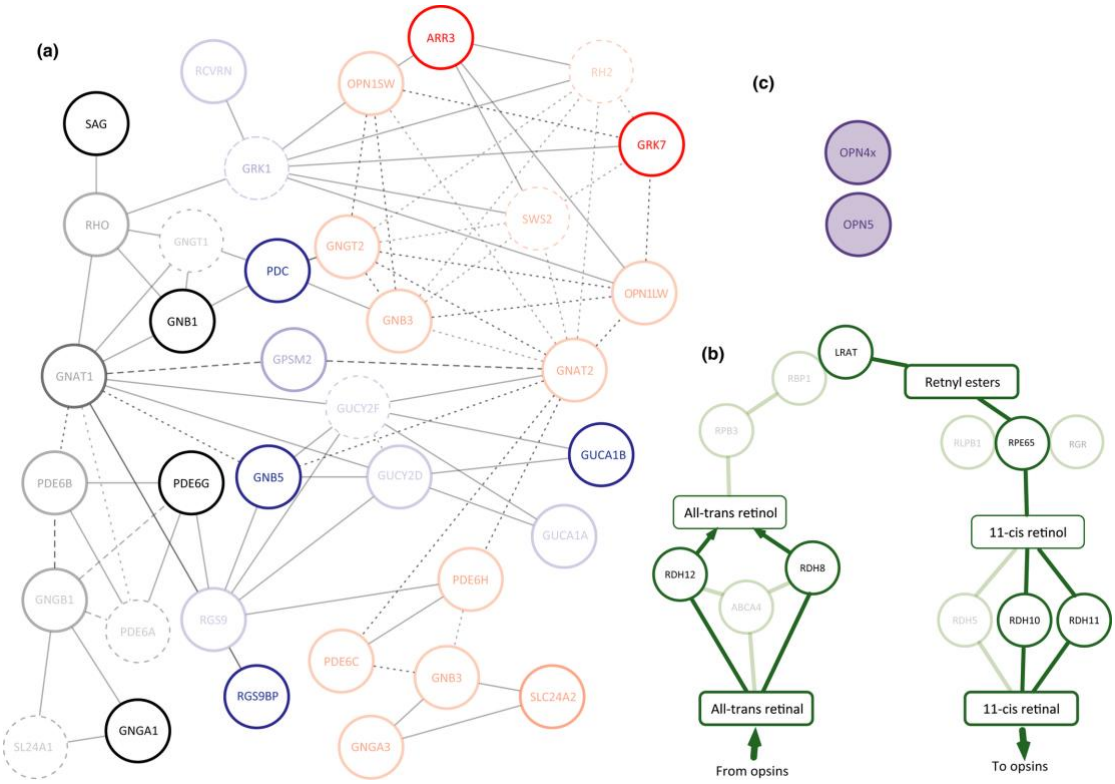

Figure 5. Visual and non-visual phototransduction pathways; highlighted genes are expressed in the sea snake skin tissue. A) Vertebrate phototransduction pathways specific to rod photoreceptors (black circles), cone photoreceptors (red circles) and both rods and cones (blue circles). Genes absent in snake genomes are also indicated (dashed line) and the visual genes present in eye but absent in skin transcriptomes are faded. B) The retinoid regeneration pathway (green circles). C) Non-visual opsins found in both putative phototactic and non-phototactic sea snake skin (shaded purple). Diagrams modified from Fu (2015); Invergo, Montanucci, Laayouni, & Bertranpetit (2013); Saari (2012).

References

Aird, S.D. et al., 2017. Population genomic analysis of a pitviper reveals microevolutionary forces underlying venom chemistry. *Genome Biology and Evolution*, 9(10), pp.2640–2649.

Alder, K., 1976. Extraocular photoreception in amphibians. *Photochemistry and Photobiology*, 23, pp.275–298.

Altschul, S.F. et al., 1990. Basic local alignment search tool. *Journal of Molecular Biology*, 215(3), pp.403–410. Available at: http://www.sciencedirect.com/science/article/pii/S0022283605803602.

Andrews, S., 2010. FastQC: a quality control tool for high throughput sequence data. Available at: http://www.bioinformatics.babraham.ac.uk/projects/fastqc.

Aubret, F. & Shine, R., 2008. The origin of evolutionary innovations: locomotor consequences of tail shape in aquatic snakes. *Functional Ecology*, 22(2), pp.317–322.

Baker, G.E. et al., 2015. Light sensitivity in a vertebrate mechanoreceptor? *The Journal of experimental biology*, 218(18), pp.2826–2829.

Ban, E. et al., 2005. The signaling pathway in photoresponses that may be mediated by visual pigments in erythrophores of Nile tilapia. *Pigment Cell Research*, 18(5), pp.360–369. Available at: http://dx.doi.org/10.1111/j.1600-0749.2005.00267.x.

Bellingham, J. et al., 2006. Evolution of melanopsin photoreceptors: Discovery and characterization of a new melanopsin in nonmammalian vertebrates. *PLoS Biology*, 4(8), pp.1334–1343.

Bertolesi, G.E. & McFarlane, S., 2018. Seeing the light to change colour: An evolutionary perspective on the role of melanopsin in neuroendocrine circuits regulating light-mediated skin pigmentation. *Pigment Cell and Melanoma Research*, 31(3), pp.354–373.

Bhattacharyya, N. et al., 2017. Cone-like rhodopsin expressed in the all-cone retina of the colubrid pine snake as a potential adaptation to diurnality. *Journal of Experimental Biology*, pp.2418–2425.

Binder, T.R. & McDonald, D.G., 2008. The role of dermal photoreceptors during the sea lamprey (*Petromyzon marinus*) spawning migration. *Journal of Comparative Physiology A: Neuroethology, Sensory, Neural, and Behavioral Physiology*, 194(11), pp.921–928.

Bretz, F. & Westfall, T.H.P., 2014. *Multiple Comparisons Using R*, Available at: https://books.google.de/books?id=U8Xc9zujgcsC.

Buhr, E.D. et al., 2015. Neuropsin (OPN5)-mediated photoentrainment of local circadian oscillators in mammalian retina and cornea. *Proceedings of the National Academy of Sciences*, 112(42), pp.13093–13098. Available at: http://www.pnas.org/lookup/doi/10.1073/pnas.1516259112.

Camacho, C. et al., 2009. BLAST+: architecture and applications. *BMC Bioinformatics*, 10, p.421. Available at: http://www.ncbi.nlm.nih.gov/pmc/articles/PMC2803857/.

Chen, S.C., Robertson, R.M. & Hawryshyn, C.W., 2013. Possible involvement of cone opsins in distinct photoresponses of intrinsically photosensitive dermal chromatophores in *Tilapia Oreochromis niloticus*. *PLoS ONE*, 8(8), pp.1–9.

Coordinators, N.R., 2016. Database resources of the National Center for Biotechnology Information. *Nucleic Acids Research*, 44(D1), pp.D7–D19. Available at: http://dx.doi.org/10.1093/nar/gkv1290.

Currie, S.P., Doherty, G.H. & Sillar, K.T., 2016. Deep-brain photoreception links luminance detection to motor output in *Xenopus* frog tadpoles. *Proceedings of the National Academy of Sciences*, 113(21), pp.6053–6058. Available at: http://www.pnas.org/lookup/doi/10.1073/pnas.1515516113.

Davies, W.I.L. et al., 2009. Shedding light on serpent sight: the visual pigments of Henophidian snakes. *Journal of Neuroscience*, 29(23), pp.7519–7525. Available at: http://www.jneurosci.org/cgi/doi/10.1523/JNEUROSCI.0517-09.2009.

Davies, W.I.L., Foster, R.G. & Hankins, M.W., 2014. The evolution and function of melanopsin in craniates. In D. M. Hunt et al., eds. *Evolution of Visual and Non-visual Pigments*. Boston, MA: Springer US, pp. 23–63. Available at: https://doi.org/10.1007/978-1-4614-4355-1_2.

Deliagina, T. et al., 1995. Initiation of locomotion by lateral line photoreceptors in lamprey: behavioural and neurophysiological studies. *The Journal of Experimental Biology*, 198(12), pp.2581–91. Available at: http://www.ncbi.nlm.nih.gov/pubmed/9320511.

Díaz, N.M., Morera, L.P. & Guido, M.E., 2016. Melanopsin and the non-visual photochemistry in the inner retina of vertebrates. *Photochemistry and Photobiology*,

687 92(1), pp.29–44.

688 Edgar, R.C., 2004. MUSCLE: multiple sequence alignment with high accuracy and high
689 throughput. *Nucleic Acids Research*, 32(5), pp.1792–1797. Available at:
690 http://dx.doi.org/10.1093/nar/gkh340.

691 Foster, R.G. & Soni, B.G., 1998. Extraretinal photoreceptors and their regulation of temporal
692 physiology. *Reviews of Reproduction*, 3(3), pp.145–150. Available at:
693 http://eutils.ncbi.nlm.nih.gov/entrez/eutils/elink.fcgi?dbfrom=pubmed&id=9829548&ret
694 mode=ref&cmd=prlinks%5Cnpapers3://publication/uuid/276F1AAB-716D-45B2-
695 86ED-B9BE5E6F773E.

696 Fu, Y., 2015. Phototransduction in rods and cones. *Webvision*, pp.1–29. Available at:
697 http://webvision.med.utah.edu/book/part-v-phototransduction-in-rods-and-
698 cones/phototransduction-in-rods-and-cones/ [Accessed April 5, 2016].

699 Fulgione, D. et al., 2014. Seeing through the skin: dermal light sensitivity provides cryptism
700 in moorish gecko. *Journal of Zoology*, 294(2), pp.122–128. Available at:
701 http://dx.doi.org/10.1111/jzo.12159.

702 Grabherr, M.G. et al., 2011. Full-length transcriptome assembly from RNA-Seq data without
703 a reference genome. *Nature Biotechnology*, 29(7), pp.644–652.

704 Graham, D.M. et al., 2008. Melanopsin ganglion cells use a membrane-associated
705 rhabdomeric phototransduction cascade. *Journal of Neurophysiology*, 99(5), pp.2522–
706 2532. Available at: https://doi.org/10.1152/jn.01066.2007.

707 Gurevich, A. et al., 2013. QUAST: quality assessment tool for genome assemblies.
708 *Bioinformatics*, 29(8), pp.1072–1075. Available at:
709 http://dx.doi.org/10.1093/bioinformatics/btt086.

710 Haas, B.J. et al., 2013. De novo transcript sequence reconstruction from RNA-seq using the
711 Trinity platform for reference generation and analysis. *Nature Protocols*, 8(8), pp.1494–
712 1512.

713 Hart, N.S. et al., 2012. Photoreceptor types, visual pigments, and topographic specializations
714 in the retinas of hydrophiid sea snakes. *J Comp Neurol*, 520(6), pp.1246–1261.
715 Available at: http://www.ncbi.nlm.nih.gov/pubmed/22020556.

716 Hauzman, E. et al., 2017. Daily activity patterns influence retinal morphology, signatures of
717 selection, and spectral tuning of opsin genes in colubrid snakes. *BMC Evolutionary*
718 *Biology*, 17(1), pp.1–14.

719 Heatwole, H., 1975. Predation on sea snakes. In W. A. Dunson, ed. *The biology of sea snakes*.
720 Baltimore: University Park Press, pp. 233–249.

721 Invergo, B. et al., 2013. A system-level, molecular evolutionary analysis of mammalian
722 phototransduction. *BMC Evolutionary Biology*, 13(1), p.52. Available at:
723 http://www.biomedcentral.com/1471-2148/13/52.

724 Isoldi, M.C. et al., 2005. Rhabdomeric phototransduction initiated by the vertebrate
725 photopigment melanopsin. *Proceedings of the National Academy of Sciences*, 102(4),
726 pp.1217–1221. Available at: http://www.pnas.org/cgi/doi/10.1073/pnas.0409252102.

727 Kearse, M. et al., 2012. Geneious Basic: An integrated and extendable desktop software
728 platform for the organization and analysis of sequence data. *Bioinformatics*, 28(12),
729 pp.1647–1649.

730 Kelley, J.L. & Davies, W.I.L., 2016. The biological mechanisms and behavioral functions of
731 opsin-based light detection by the skin. *Front. Ecol. Evol*, 4(4), pp.1063389–106.

732 Kingston, A.C.N. et al., 2015. Visual phototransduction components in cephalopod

chromatophores suggest dermal photoreception. *The Journal of Experimental Biology*, 218(10), pp.1596–1602. Available at: http://jeb.biologists.org/content/218/10/1596%5Cnhttp://jeb.biologists.org/content/218/10/1596.abstract?etoc%5Cnhttp://jeb.biologists.org/content/218/10/1596.full.pdf.

Kingston, A.C.N. & Cronin, T.W., 2016. Diverse distributions of extraocular opsins in crustaceans, cephalopods, and fish. *Integrative and Comparative Biology*, 56(5), pp.820–833.

Kolde, R., 2012. Pheatmap: pretty heatmaps. Available at: http://cran.r-project.org/web/packages/pheatmap/pheatmap.pdf.

Langmead, B. & Salzberg, S.L., 2012. Fast gapped-read alignment with Bowtie 2. *Nature Methods*, 9, p.357. Available at: http://dx.doi.org/10.1038/nmeth.1923.

Lex, A., Gehlenborg, N. & Strobelt, H., 2016. UpSet: visualization of intersecting sets. *Europe PMC Funders Group*, 20(12), pp.1983–1992.

Masunaga, G. et al., 2008. Shark predation of sea snakes (Reptilia: Elapidae) in the shallow waters around the Yaeyama Islands of the southern Ryukyus, Japan. *Marine Biodiversity Records*, 1, p.e96.

Mäthger, L.M., Roberts, S.B. & Hanlon, R.T., 2010. Evidence for distributed light sensing in the skin of cuttlefish, Sepia officinalis. *Biology Letters*, 6(April), pp.600–603. Available at: http://www.pubmedcentral.nih.gov/articlerender.fcgi?artid=2936158&tool=pmcentrez&rendertype=abstract.

Matynia, A. et al., 2016. Peripheral sensory neurons expressing melanopsin respond to light. *Frontiers in Neural Circuits*, 10(August), pp.1–15. Available at: http://journal.frontiersin.org/Article/10.3389/fncir.2016.00060/abstract.

Millott, N., 1968. The dermal light sense. *Symposia of the Zoological Society of London*, 23, pp.1–36.

Mirtschin, P., Rasmussen, A. & Weinstein, S., 2017. *Dangerous snakes of Australia: identification, biology and envenoming* 1st ed., Clayton, Victoria: CSIRO Publishing.

Moriya, T. et al., 1996. Light-sensitive response in melanophores of *Xenopus laevis*: I. Spectral characteristics of melanophore response in isolated tail fin of *Xenopus* tadpole. *Journal of Experimental Zoology*, 276(1), pp.11–18.

Newth, D.R. & Ross, D.M., 1954. On the reaction to light of *Myxine Clutinosa L. The Journal of Experimental Biology*, 32, pp.4–21.

Nitschke, C.R. et al., 2018. Rates of population differentiation and speciation are decoupled in sea snakes. *Biology letters*, 14(10), p.20180563. Available at: http://www.ncbi.nlm.nih.gov/pubmed/30333264.

O'Leary, N.A. et al., 2016. Reference sequence (RefSeq) database at NCBI: current status, taxonomic expansion, and functional annotation. *Nucleic Acids Research*, 44(D1), pp.D733–D745. Available at: http://dx.doi.org/10.1093/nar/gkv1189.

Oshima, N., 2001. Direct reception of light by chromatophores of lower vertebrates. *Pigment Cell Research*, 14(5), pp.312–319.

Patro, R. et al., 2017. Salmon provides fast and bias-aware quantification of transcript expression. *Nature Methods*, 14(4), pp.417–419. Available at: http://dx.doi.org/10.1038/nmeth.4197.

Patzner, R.A., 1978. Experimental studies on the light sense in the hagfish, *Eptatretus burgeri* and *Paramyxine atami* (Cyclostomata). *Helgoländer Wissenschaftliche*

Meeresuntersuchungen, 31(1–2), pp.180–190. Available at: http://www.scopus.com/inward/record.url?eid=2-s2.0-1542601226&partnerID=40&md5=cfdf0c4834a993560022de5a76f7a14f.

Pearse, A.S., 1910. The reactions of amphibians to light. *Proceedings of the American Academy of Arts and Sciences*, 45(6), pp.161–208.

Peirson, S.N., Halford, S. & Foster, R.G., 2009. The evolution of irradiance detection: melanopsin and the non-visual opsins. *Philosophical Transactions of the Royal Society of London B: Biological Sciences*, 364(1531), pp.2849–2865. Available at: http://rstb.royalsocietypublishing.org/content/364/1531/2849.abstract.

Porter, M.L. et al., 2011. Shedding new light on opsin evolution. *Proceedings of the Royal Society of London B: Biological Sciences*, 279, pp.3–14.

Provencio, I. et al., 1998. Melanopsin: An opsin in melanophores, brain, and eye. *Proc Natl Acad Sci U S A*, 95(1), pp.340–345. Available at: http://www.ncbi.nlm.nih.gov/pubmed/9419377%5Cnhttp://www.ncbi.nlm.nih.gov/pmc/articles/PMC18217/pdf/pq000340.pdf.

Provencio, I. & Warthen, D.M., 2012. Melanopsin, the photopigment of intrinsically photosensitive retinal ganglion cells. *Wiley Interdisciplinary Reviews: Membrane Transport and Signaling*, 1(2), pp.228–237.

Ramirez, M.D. et al., 2011. Understanding the dermal light sense in the context of integrative photoreceptor cell biology. *Visual Neuroscience*, 28, pp.265–279.

Ramirez, M.D. & Oakley, T.H., 2015. Eye-independent, light-activated chromatophore expansion (LACE) and expression of phototransduction genes in the skin of Octopus bimaculoides. *The Journal of Experimental Biology*, 218, pp.1513–1520.

Rasmussen, A.R. et al., 2011. Marine reptiles. *PLOS one*, 6(11), p.e27373.

R Core Team, 2017. R: A language and environment for statistical computing. Available at: https://www.r-project.org/.

Reese, A.M., 1906. Observation on the reactions of *Cryptobranchus* and *Necturus* to light and heat. *The Biological Bulletin*, 11, pp.93–99.

Robinson, M.D., McCarthy, D.J. & Smyth, G.K., 2009. edgeR: A Bioconductor package for differential expression analysis of digital gene expression data. *Bioinformatics*, 26(1), pp.139–140.

Ronan, M. & Bodznick, D., 1991. Behavioral and neurophysiological demonstration of a lateralis skin photosensitivity in larval sea lampreys. *Journal of Experimental Biology*, 161, pp.97–117. Available at: http://jeb.biologists.org/content/161/1/97.abstract.

Saari, J.C., 2012. Vitamin A metabolism in rod and cone visual cycles. *Annual Review of Nutrition*, 32(1), pp.125–145.

Sanders, K.L., Rasmussen, A.R. & Elmberg, J., 2012. Independent innovation in the evolution of paddle-shaped tails in viviparous sea snakes (Elapidae: Hydrophiinae). *Integrative and Comparative Biology*, 52(2), pp.311–320. Available at: http://icb.oxfordjournals.org/content/52/2/311.abstract.

Sayle, M.H., 1916. The reactions of *Necturus* to stimuli received through the skin. *J Anim Behav*, 6(2), pp.81–102.

Schott, R. et al., 2017. Targeted capture of complete coding regions across divergent species. *bioRxiv*.

Schott, R.K. et al., 2015. Evolutionary transformation of rod photoreceptors in the all-cone retina of a diurnal garter snake. *Proceedings of the National Academy of Sciences of the*

United States of America, 113(2), pp.356–361. Available at: http://www.ncbi.nlm.nih.gov/pubmed/26715746.

Schubert, M., Lindgreen, S. & Orlando, L., 2016. AdapterRemoval v2: Rapid adapter trimming, identification, and read merging. *BMC Research Notes*, 9(1), pp.1–7.

Schweikert, L.E., Fitak, R.R. & Johnsen, S., 2018. De novo transcriptomics reveal distinct phototransduction signaling components in the retina and skin of a color-changing vertebrate, the hogfish (*Lachnolaimus maximus*). *Journal of Comparative Physiology A*, 0(0), pp.1–11. Available at: http://link.springer.com/10.1007/s00359-018-1254-4.

Sherratt, E., Rasmussen, A.R. & Sanders, K.L., 2018. Trophic specialization drives morphological evolution in sea snakes. *Royal Society Open Science*, 5(3), p.172141.

Simões, B.F. et al., 2016. Visual pigments, ocular filters and the evolution of snake vision. *Molecular Biology and Evolution*, 33(10), p.msw148. Available at: http://mbe.oxfordjournals.org/lookup/doi/10.1093/molbev/msw148.

Stamatakis, A., 2006. RAxML-VI-HPC: maximum likelihood-based phylogenetic analyses with thousands of taxa and mixed models. *Bioinformatics*, 22(21), pp.2688–2690. Available at: http://dx.doi.org/10.1093/bioinformatics/btl446.

Steven, D.M., 1955. Experiments on the light sense of the hag, *Myxine glutinosa L*. *Journal of Experimental Biology*, 32(1), p.22. Available at: http://jeb.biologists.org/cgi/content/abstract/32/1/22.

Steven, D.M., 1950. Some properties of the photoreceptors of the brook lamprey. *Journal of Experimental Biology*, 27(3), p.350. Available at: http://jeb.biologists.org/cgi/content/abstract/27/3/350.

Steven, D.M., 1963. The dermal light sense. *Biological Reviews*, 38, pp.204–240.

The UniProt Consortium, 2017. UniProt: the universal protein knowledgebase. *Nucleic Acids Research*, 45(D1), pp.D158–D169. Available at: http://dx.doi.org/10.1093/nar/gkw1099.

Torsten, H., Frank, B. & Peter, W., 2008. Simultaneous inference in general parametric models. *Biometrical Journal*, 50(3), pp.346–363. Available at: https://doi.org/10.1002/bimj.200810425.

Tu, D.C. et al., 2006. Inner retinal photoreception independent of the visual retinoid cycle. *Proceedings of the National Academy of Sciences*, 103(27), pp.10426–10431. Available at: http://www.pnas.org/cgi/doi/10.1073/pnas.0600917103.

Ullén, F. et al., 1993. Role of dermal photoreceptors and lateral eyes in initiation and orientation of locomotion in lamprey. *Behavioural Brain Research*, 54(1), pp.107–110.

Ward, C.M., To, H. & Pederson, S.M., 2018. ngsReports: An R Package for managing FastQC reports and other NGS related log files. *bioRxiv*, p.313148. Available at: http://biorxiv.org/content/early/2018/05/02/313148.abstract.

Wolken, J.J., 1995. Light that controls behavior: extraocular photoreception. In J. J. Wolken, ed. *Light detectors, photoreceptors, and imaging systems in nature*. New York: Oxford University Press, pp. 191–204.

Wolken, J.J., 1988. Photobehavior of marine invertebrates: extraocular photoreception. *Comparative Biochemistry and Physiology*, 91C(1), pp.145–149.

Wright, C.B., Redmond, T.M. & Nickerson, J.M., 2015. *A history of the classical visual cycle* 1st ed., Elsevier Inc. Available at: http://dx.doi.org/10.1016/bs.pmbts.2015.06.009.

Young, J.Z., 1935. The photoreceptors of lampreys 1. Light sensitive fibres in the lateral line nerves. *The Journal of Experimental Biology*, 12, pp.229–238.

870 Zeilies, A., Kleiber, C. & Jackman, S., 2008. Regression models for count data in R. *Journal*
871 *of Statistical Software*, 27(8), pp.1–25. Available at: http://www.jstatsoft.org/v27/i08.

872 Zimmerman, K. & Heatwole, H., 1990. Cutaneous photoreception: a new sensory mechanism
873 for reptiles. *Copeia*, 1990(3), pp.860–862.

874

875